JOURNAL OF SYNCHROTRON RADIATION

ISSN 1600-5775

Optical performance of materials for X-ray refractive optics in the energy range 8–100 keV

Dmitry Serebrennikov,[a]* Evgeny Clementyev,[a,b] Alexander Semenov[c] and Anatoly Snigirev[a]

[a]I. Kant Baltic Federal University, Nevskogo 14 A, Kaliningrad 236041, Russian Federation, [b]Institute for Nuclear Research (INR), Prospekt 60-Letiya Oktyabrya, Mosow 117312, Russian Federation, and [c]A. A. Bochvar High-Technology Scientific Research Institute for Inorganic Materials, Rogova str. 5a, Moscow 123098, Russian Federation. *Correspondence e-mail: dserebrennikov@innopark.kantiana.ru

Received 3 May 2016
Accepted 13 September 2016

Edited by Y. Amemiya, University of Tokyo, Japan

Keywords: X-ray optics; refractive lenses; X-ray windows; optical performance.

A quantitative analysis of the crucial characteristics of currently used and promising materials for X-ray refractive optics is performed in the extended energy range 8–100 keV. According to the examined parameters, beryllium is the material of choice for X-ray compound refractive lenses (CRLs) in the energy range 8–25 keV. At higher energies the use of CRLs made of diamond and the cubic phase of boron nitride (c-BN) is beneficial. It was demonstrated that the presence of the elements of the fourth (or higher) period has a fatal effect on the functional X-ray properties even if low-Z elements dominate in the compound, like in YB_{66}. Macroscopic properties are discussed: much higher melting points and thermal conductivities of C and c-BN enable them to be used at the new generation of synchrotron radiation sources and X-ray free-electron lasers. The role of crystal and internal structure is discussed: materials with high density are preferable for refractive applications while less dense phases are suitable for X-ray windows. Single-crystal or amorphous glass-like materials based on Li, Be, B or C that are free of diffuse scattering from grain boundaries, voids and inclusions are the best candidates for applications of highly coherent X-ray beams.

1. Introduction.

The rapid development of X-ray investigation techniques has contributed to the emergence of a wide variety of X-ray optics, including windows, filters, monochromators, pinholes and focusing optics. In turn, focusing X-ray optics can be roughly divided into three groups based on the physical principle of generating a small focus spot. The first group is based on reflection and includes curved mirrors, multilayers and capillaries. The second group consists of Fresnel zone plates and is founded on diffraction. The last group is based on refraction and comprises X-ray compound refractive lenses (CRLs) (Snigirev *et al.*, 1996). Presently, CRLs have become widely used due to their relative simplicity. The first demonstration of focusing X-rays by CRLs made by drilling arrays of cylindrical holes in aluminium was performed by Snigirev in 1996 and gave rise to further development of X-ray refractive lenses. In particular, some works concerned the study of the lens shape (kinoform, elliptical, spherical and parabolic), maximum length of the CRL (Kohn, 2003) and, of course, lens materials. Up to now, lenses made of beryllium, diamond, aluminium, silicon, nickel and some polymers have been studied. In terms of absorption, beryllium is considered to be the best material for manufacturing CRLs. Application of lenses made of beryllium instead of aluminium has increased the flux in the

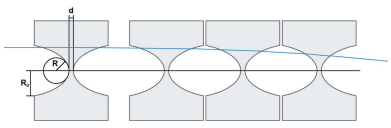

X-ray microbeam by at least one order of magnitude at energies below 30 keV (Schroer *et al.*, 2002). Nevertheless, beryllium has some essential disadvantages, such as toxicity, degradation (oxidation) and difficulties in parabolic surface treatment. Furthermore, due to relatively low refraction of beryllium, CRLs demand a significant number of elementary lenses to provide short focus length. This fact is of special importance in the context of the X-ray transfocator. This device comprises a lens assembly whose focal distance can be continuously adjusted by mechanical movement of one or more groups of individual lenses (Snigirev *et al.*, 2009). In order to reduce the length of the transfocator, the number of elementary lenses should be minimized. This can be achieved by applying materials with a refractive ability higher than beryllium, whereas transmission should be kept as high as possible.

The new generation of synchrotron radiation sources with significantly increased beam brilliance but high thermal load makes additional requirements for lens materials, such as high melting point, thermal conductivity, chemical stability and low thermal expansion coefficient. Optics that should be resilient to extra high thermal and radiation loading are also required for X-ray free-electron lasers, which are expected to be the most powerful X-ray source. In light of this, materials with strong covalent bonding like diamond or the cubic modification of boron nitride, where sp^3-hybridization is observed, look promising and should be studied in more detail.

This article presents an analysis of promising materials for X-ray CRLs in the energy range 8–100 keV and comparison with commonly used materials. Special attention is paid to binary chemical compounds, which have never been investigated before in relation to X-ray optics. Since X-ray windows as well as CRLs require high transmission, we also define materials which can be applied to X-ray windows. In addition, the presence of elements with high atomic number in binary compounds with high concentration of the second light element and its influence on X-ray properties is discussed. The role of internal structure is also studied. Finally, according to the defined criteria, analysis of optimal materials for X-ray lenses in the energy range 8–100 keV is performed.

2. Atomic properties

The interaction of X-rays with condensed matter may be described through the index of refraction n,

$$n = 1 - \delta + i\beta, \tag{1}$$

where δ is the decrement of the refractive index and β is the absorption coefficient. Both values can be obtained from the scattering factor $f = Z + f' + if''$, where Z is the atomic number and $f' + if''$ is the dispersion correction (Henke *et al.*, 1993). In this case the decrement of the refractive index can be written as

$$\delta = \frac{r_0 N_A}{2\pi} \lambda^2 \rho \frac{Z + f'}{A}, \tag{2}$$

where r_0 is the classical electron radius, N_A is Avogadro's number, λ is the photon wavelength, A is the atomic mass and ρ is the density of the material (Tummler, 2000). The decrement of the refractive index for binary compound X_kY_h is given by

$$\delta = \frac{r_0 N_A}{2\pi} \lambda^2 \rho_c \frac{k(Z_X + f'_X) + h(Z_Y + f'_Y)}{kA_X + hA_Y}, \tag{3}$$

where ρ_c is the density of the compound X_kY_h.

The absorption coefficient for a single element is given by

$$\beta = \frac{r_0 N_A}{2\pi} \lambda^2 \rho \frac{f''}{A}. \tag{4}$$

For binary compound X_kY_h we may rewrite equation (4) as

$$\beta = \frac{r_0 N_A}{2\pi} \lambda^2 \rho_c \frac{kf''_X + hf''_Y}{kA_X + hA_Y}. \tag{5}$$

The decrement of the refractive index describes the strength of refraction with respect to a vacuum. In turn, the absorption coefficient defines the part of the energy that will be absorbed by the material. The absorption coefficient is related to the attenuation coefficient μ_a as (Lengeler *et al.*, 1999)

$$\beta = \frac{\lambda \mu_a}{4\pi}. \tag{6}$$

It should be noted that energy losses are caused not only by absorption in material. The total linear attenuation coefficient can be written as the sum over the contribution from absorption, coherent (Rayleigh's) and incoherent (Compton's) scattering,

$$\mu = \mu_a + \mu_\kappa + \mu_p. \tag{7}$$

For binary compound X_kY_h the total linear attenuation coefficient is given by

$$\mu = \rho_c \frac{kA_X \mu_{mX} + hA_Y \mu_{mY}}{kA_X + hA_Y}, \tag{8}$$

where μ_{mX} and μ_{mY} are the mass-attenuation coefficients of elements X and Y, respectively.

Among a wide range of X-ray optics the majority require high transmission, which can be obtained by applying materials with low linear attenuation coefficient. Values of the linear attenuation coefficients of some promising and commonly used materials in the energy range 8–100 keV are listed in Table 1 [mass attenuation coefficients were taken from the online NIST database (http://srdata.nist.gov/) and Henke *et al.* (1993)].

As seen from Table 1, the linear attenuation coefficient grows larger as the material atomic number increases. In light of this only elements of the second and third periods of the periodic table and their compounds can be used as functional materials for X-ray optics, which require high transmission. With regard to the listed materials, the lowest linear attenuation coefficient are for Be, B_4C, LiB, AlB_{12}, C (hereafter we consider only the diamond phase), BN [hereafter we consider only the cubic phase of boron nitride (c-BN)] and

Table 1
Linear attenuation coefficients in the energy range 8–100 keV.

	μ (mm^{-1})							
Material	8 keV	10 keV	15 keV	20 keV	25 keV	30 keV	50 keV	100 keV
Be	0.21	0.12	0.06	0.04	0.04	0.03	0.03	0.02
B_4C	0.69	0.37	0.14	0.08	0.06	0.05	0.04	0.03
AlB_{12}	2.72	1.42	0.45	0.22	0.13	0.09	0.05	0.04
C	1.59	0.8	0.28	0.15	0.11	0.09	0.07	0.05
c-BN	1.82	0.94	0.31	0.17	0.1	0.09	0.06	0.05
Al	13.59	7.08	2.15	0.9	0.49	0.30	0.1	0.05
YB_{66}	4.04	2.2	0.74	1.98	1.12	0.7	0.2	0.06
Al_2O_3	12.81	6.02	2.02	0.89	0.43	0.31	0.12	0.06
SiC	14.98	7.85	2.40	1.05	0.51	0.35	0.12	0.06
LiB	0.24	0.14	0.06	0.04	0.03	0.03	0.02	0.02
LiAl	7.06	3.68	1.12	0.49	0.26	0.16	0.06	0.03
SiO_2	9.65	5.04	1.54	0.68	0.33	0.23	0.08	0.04
SU-8	1.16	0.62	0.21	0.1	0.07	0.05	0.04	0.02

Table 2
Half-value layer in the energy range 8–100 keV.

	x (mm)							
Material	8 keV	10 keV	15 keV	20 keV	25 keV	30 keV	50 keV	100 keV
Be	3.30	5.78	11.55	17.01	19.52	21.09	24.10	28.08
B_4C	1	1.89	5.11	8.52	11.79	13.03	16.55	19.96
AlB_{12}	0.26	0.49	1.53	3.22	5.34	7.42	13.46	18.74
C	0.44	0.86	2.52	4.52	6.27	7.63	10.39	13.08
c-BN	0.38	0.74	2.21	4.19	6.95	7.64	10.90	13.68
Al	0.05	0.1	0.33	0.77	1.42	2.30	6.98	14.90
YB_{66}	0.17	0.32	0.37	0.35	0.63	1.00	3.50	12.28
Al_2O_3	0.05	0.12	0.34	0.78	1.59	2.24	5.88	10.64
SiC	0.05	0.09	0.29	0.66	1.36	1.99	5.94	12.42
LiB	2.9	5.15	12.19	18.04	22.74	24.3	28.96	34.2
LiAl	0.09	0.18	0.60	1.39	2.61	4.14	11.92	23.78
SiO_2	0.07	0.14	0.45	1.03	2.1	3	8.21	15.53
SU-8	0.6	1.12	3.37	6.73	10.63	14.4	16.09	30.71

SU-8. Linear attenuation coefficients of other materials are an order of magnitude higher.

Practically, it is more convenient to use the half-value layer instead of the linear attenuation coefficient. The half-value layer is the length of material where the initial intensity is reduced by two times,

$$x = \frac{\ln(2)}{\mu}. \tag{9}$$

Fig. 1 and Table 2 present values of the half-value layer of the listed materials in the energy range 8–100 keV.

Besides high transmission, materials for the CRLs should provide high refraction, defined by the decrement of the refractive index. In light of this, it is reasonable to introduce a new parameter N_0, which includes both the decrement of the refractive index and the linear attenuation coefficient,

$$N_0 = \delta/\mu. \tag{10}$$

The values of refraction-to-absorption ratio N_0 of the listed materials in the energy range 8–100 keV are given in Table 3.

As shown in Table 3 and Fig. 2, all materials can be separated into two groups. The first group contains materials with high values of N_0 (Be, LiB, B_4C, C, c-BN, AlB_{12}, SU-8) in the energy range 8–40 keV; the second group consists of materials with low values of N_0 (LiAl, Al, Al_2O_3, SiC, YB_{66}, SiO_2) in the energy range 8–40 keV. Nevertheless, the refraction-to-absorption ratio of all listed materials become very similar at higher energies.

3. Refraction performance of materials

Owing to the low magnitude of the decrement of the refractive index a single X-ray lens has an extremely long focus distance. This problem can be solved by using X-ray CRLs made up of a long row of elementary lenses (Snigirev *et al.*, 1996). In this case, the focus distance of a CRLs consisting of N elements is defined as

$$f = R/2\delta N, \tag{11}$$

where R is the radius of curvature at the apex of the parabolas (Fig. 3).

As follows from the equation above, the number of necessary elements N in the CRL depends on the choice of material as well, $N = R/2\delta f$. By fixing the focus length (1 m) and radius of curvature at the apex of the parabolas (0.05 mm) we can estimate this parameter. The results are presented in Table 4.

These results are of great importance. As shown in Fig. 4, Al_2O_3, C, c-BN, SiC, Al_2O_3, AlB_{12}, Al, YB_{66} and SiO_2 demonstrate better refraction than other materials and require fewer individual lenses in the CRL. At the same time, leading by the most parameters beryllium requires almost two times more lenses than, for example, diamond.

The main parameter defining the optical performance of the lens is the effective aperture. To a first approximation, the

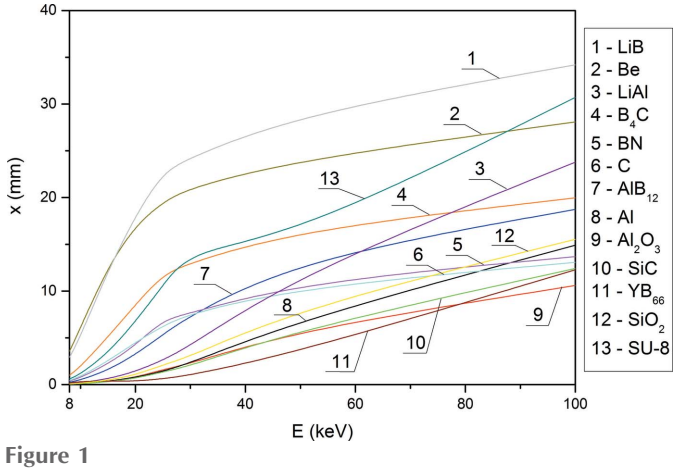

Figure 1
Half-value layer in the energy range 8–100 keV.

Table 3
Refraction-to-absorption ratio N_0 in the energy range 8–100 keV.

	N_0 ($\times 10^{-7}$) (mm)							
Material	8 keV	10 keV	15 keV	20 keV	25 keV	30 keV	50 keV	100 keV
Be	273.5	300.4	276.5	209.3	153.9	115.3	47.51	13.81
B_4C	108.13	130.66	157.1	147.2	130.3	100	45.73	13.79
AlB_{12}	28.63	34.94	48.68	57.51	61.09	58.94	38.47	13.39
C	74.38	91.08	117.8	119	106	89.07	43.75	13.74
c-BN	59.54	73.58	98.42	104.65	111.2	84.88	43.6	13.67
Al	6.46	7.93	12.99	15.04	17.71	19.9	21.74	11.57
YB_{66}	18.65	21.87	28.61	6.06	6.88	7.68	9.71	8.53
Al_2O_3	10.02	13.61	17.91	22.91	30.04	29.23	27.61	12.48
SiC	7.03	8.56	12.37	15.94	20.94	21.3	22.84	11.91
LiB	180.1	208.9	219.5	182.8	147.4	109.5	46.93	13.86
LiAl	7.73	9.45	13.73	17.71	21.28	23.41	24.27	12.1
SiO_2	9	11.01	15.94	20.41	26.73	26.44	26.05	12.32
SU-8	36.83	44.26	58.78	66.07	66.75	62.73	25.27	12.06

aperture of the lens is $2R$. However, high absorption near the edges of the lens limits the effective aperture to

$$D_{\rm eff} = 2R_0\left[\frac{1-\exp(-a)}{a}\right]^{1/2}, \quad (12)$$

$$a = \frac{\mu N R_0^2}{2R}, \quad (13)$$

where $2R_0$ is the geometrical aperture, R is the radius of curvature at the apex of the parabolas (Fig. 3), μ is the linear attenuation coefficient and N is the number of elementary lenses. Here we neglect the roughness of the lens surface.

In fact, the optical performance of a CRL is characterized by two parameters: gain and diffraction-limited resolution of the lens. According to the theory of imaging with a parabolic continuously refractive X-ray lens (Kohn, 2003), both parameters are defined mainly by the effective aperture.

Effective apertures of listed materials in the energy range 8–100 keV are given in Table 5.

As seen from Fig. 5, beryllium has the best aperture among all examined materials. In the energy range 8–25 keV the difference in effective aperture values between beryllium and other materials is essential; however, at higher energies it turns out to be insignificant, especially for LiB, B_4C, C and c-BN.

In terms of the gain and the diffraction limit, beryllium provides the best performance as long as it has the highest effective aperture. However, as was mentioned before, it requires too many lenses. Thus, it is reasonable to introduce a new indicator called the refraction performance, $D_{\rm eff}^2/N$. Fig. 6 shows the refraction performance of diamond, the cubic phase of boron nitride and aluminium in relation to beryllium (which is assumed to be unity at all energies in Fig. 6).

The superiority of diamond and the cubic modification of boron nitride against beryllium is caused by the similar effective apertures on the one hand and significant difference in number of required elementary lenses on the other. The refraction performance of aluminium, which represents materials with relatively low effective aperture, is competitive with beryllium starting from approximately 65 keV but is still worse than diamond or cubic boron nitride. Nevertheless, due to the wide commercial availability of Al lenses it is reasonable to use them above 65 keV.

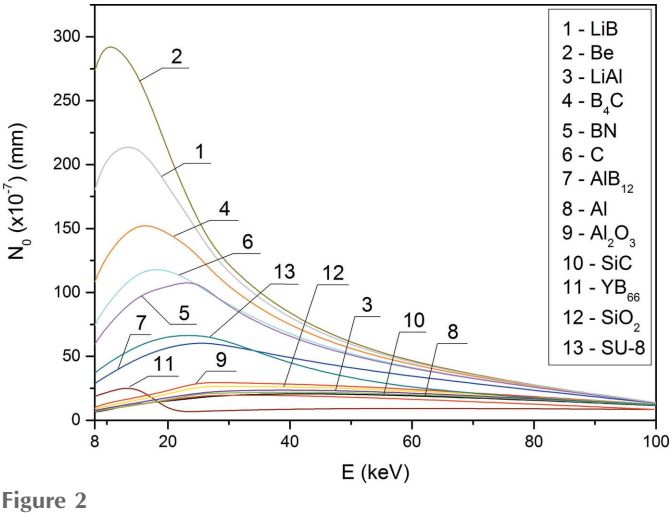

Figure 2
Refraction-to-absorption ratio N_0 in the energy range 8–100 keV.

4. The role of internal and crystal structure

Parameters of X-ray optics are not only defined by the atomic properties of the elements: internal structure plays an important part as well. Let us consider the difference in X-ray properties of one material in different phase modifications; take boron nitride, for example. It exists in various crystalline forms: hexagonal, cubic (analogous to diamond) and wurtzite phases (Solozhenko, 1995). The difference in crystal structure involves a complete reconstruction of the atomic arrangement. This leads to changing of the refractive index decrement and absorption coefficient due to density variation, while parameter N_0 keeps constant in all cases since δ and β both include ρ as follows from equations (2) and (4). As the effective aperture depends mainly on N_0, there seems to be no distinction between various states of boron nitride in terms of X-ray refractive optics. However, density is of great importance. As was mentioned above, the decrement of the refractive index can be expressed as a function of density.

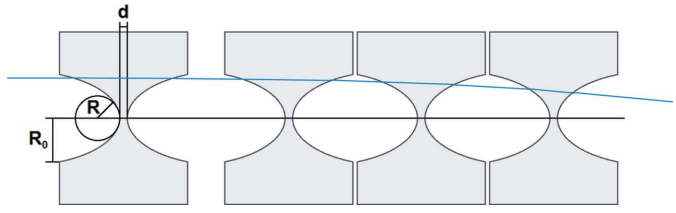

Figure 3
Compound refractive X-ray lens. Owing to the low refraction index the CRL comprises several elementary lenses. Each elementary lens has a concave profile. The blue line demonstrates the path of the X-rays in the CRL.

Table 4
Number of required lenses in the energy range 8–100 keV.

Parameters used in calculations: focal length f, 1 m; radius of curvature at the apex of parabolas R, 0.05 mm.

	N							
Material	8 keV	10 keV	15 keV	20 keV	25 keV	30 keV	50 keV	100 keV
Be	5	7	16	29	46	67	189	883
B_4C	3	5	12	21	33	47	133	522
AlB_{12}	3	5	11	20	32	45	126	505
C	2	3	8	14	21	31	86	343
c-BN	2	4	8	14	23	32	90	361
Al	3	5	10	18	29	42	118	510
YB_{66}	3	5	12	21	32	47	130	519
Al_2O_3	2	3	7	12	19	28	77	308
SiC	2	4	8	15	23	34	94	376
LiB	6	9	20	35	55	80	222	887
LiAl	5	7	16	29	45	65	181	725
SiO_2	3	5	10	18	28	41	114	455
SU-8	6	9	21	37	57	83	230	919

Table 5
Effective apertures in the energy range 8–100 keV.

Parameters used in calculations: focal length f, 1 m; radius of curvature at the apex of parabolas R, 0.05 mm; geometrical aperture $2R_0$, 0.442 mm.

	$D_{\rm eff}$ (μm)							
Material	8 keV	10 keV	15 keV	20 keV	25 keV	30 keV	50 keV	100 keV
Be	395	403	400	386	369	348	269	149
B_4C	354	362	370	366	353	337	263	149
AlB_{12}	219	235	272	286	289	288	243	146
C	318	339	346	348	342	326	256	148
c-BN	302	299	336	342	343	323	256	148
Al	100	108	139	157	169	179	188	142
YB_{66}	181	190	210	98	106	111	125	117
Al_2O_3	124	149	168	193	218	213	209	141
SiC	116	113	144	160	184	184	191	138
LiB	374	384	379	379	365	343	264	149
LiAl	106	125	149	168	185	193	196	139
SiO_2	118	126	161	181	207	204	203	140
SU-8	236	259	285	298	300	293	200	139

Indeed, an electric field of the incident X-ray wave induces an oscillating dipole moment in condensed matter upon interaction with it. This oscillating dipole moment generates an additional X-ray wave with the electric field proportional to the initial wave. Interaction of these two electric fields leads to a phase shift of the incident wave. This phase shift depends on the density of the material; therefore more dense material refracts electromagnetic waves stronger than less dense material. As can be seen from equation (11), the focus length does not take into account β or N_0 as long as only δ has influence on the refraction. Thus, by using a phase modification with higher density we may achieve a smaller focus distance and reduce the number of elementary lenses. Fig. 7 shows the number of elementary lenses required to reach a focus distance of 1 m for two different boron nitride modifications: cubic modification with density 3.41 g cm^{-3} and hexagonal modification with density 2.18 g cm^{-3} (R was fixed and was equal to 0.05 mm).

As seen in Fig. 7, we need significantly fewer lenses made of cubic boron nitride than of hexagonal, particularly at higher energies. At the same time, intensity losses are similar in both cases although c-BN has a higher absorption coefficient. From the attenuation law for an X-ray beam with intensity I_0 penetrating a layer of material with thickness d and density p, we can derive

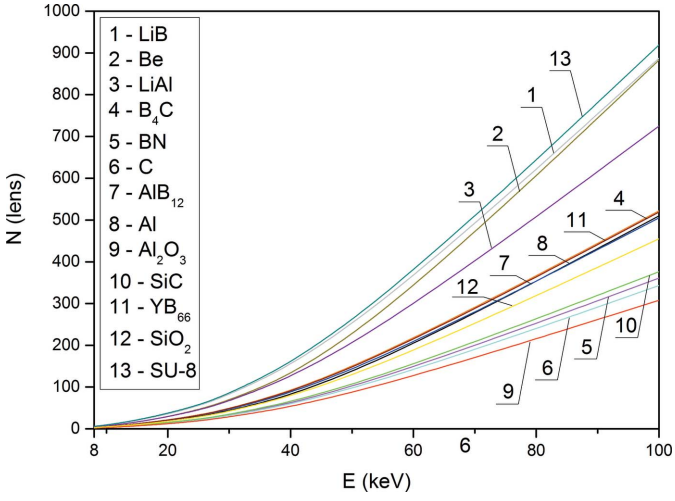

Figure 4
Number of required lenses in the energy range 8–100 keV. Parameters used in calculations: focal length f, 1 m; radius of curvature at the apex of parabolas R, 0.05 mm.

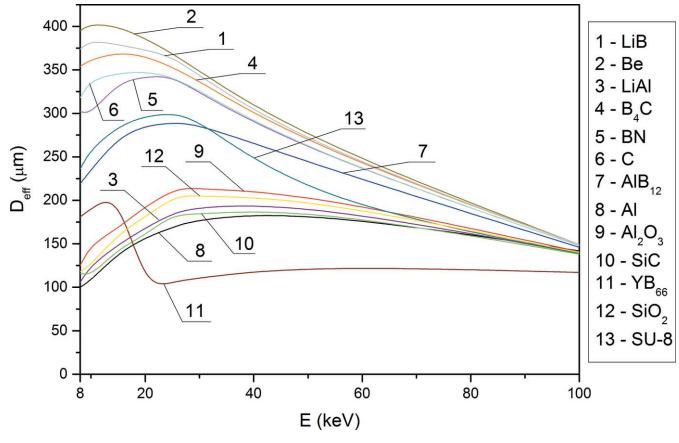

Figure 5
Effective apertures in the energy range 8–100 keV. Parameters used in calculations: focal length f, 1 m; radius of curvature at the apex of parabolas R, 0.05 mm; geometrical aperture $2R_0$, 0.442 mm.

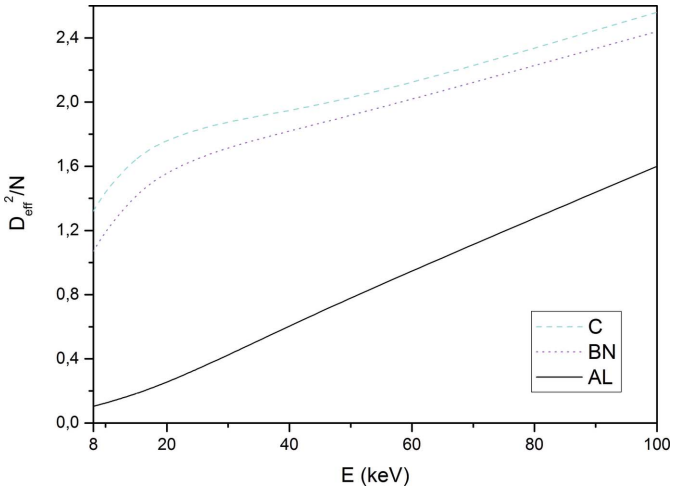

Figure 6
Refraction performance of diamond, cubic modification of boron nitride and aluminium in relation to beryllium.

$$I/I_0 = \exp(-\mu d). \quad (14)$$

The cubic modification has a higher μ value, it requires fewer lenses, and therefore the thickness of material d decreases. The hexagonal modification has a lower μ value, but requires more lenses to achieve an equal focus length, and therefore the thickness d increases. In turn, in the context of X-ray windows, high refraction is of no interest while only high transmission is required. In this case μ should be minimized and hexagonal modification becomes more preferable.

Another important aspect of material properties is the internal structure, that can be single-crystal, polycrystalline or amorphous. This feature is not connected to the crystal lattice and is based mainly on the material synthesis. Internal structure plays a critical role in the methods of investigations using X-rays that are sensitive to extra small phase objects like microscopy, radiography, *etc*. It has been shown (Lyatun *et al.*, 2015) that a polycrystalline structure with grain size higher than the coherence length significantly distorts the wavefront of an incident wave and creates a parasitic speckle structure on the image. Obviously, materials with such a grain size cannot be used either for CRLs or X-ray windows at synchrotron radiation sources. For example, Figs. 8(*a*) and 8(*b*) present SEM images of the surface of a cubic boron nitride sample that was synthesized at the Institute for High Pressure Physics (Troitsk, Russia) with the aim of studying its optical properties. As can be seen, the grain size varies in the range ~1–50 µm. In order to take a radiographic image of this sample, it was tested at beamline ID06 of the ESRF. A preliminarily polished c-BN sample of thickness 1 mm was located at 58.85 m from the undulator source. The measurements were performed at the energy 14 keV using a high-resolution X-ray CCD camera (0.73 µm pixel size) placed at 0.6 m after the sample. The radiographic image is displayed in Fig. 8(*c*). The parasitic phase contrast caused by the internal structure is observed well.

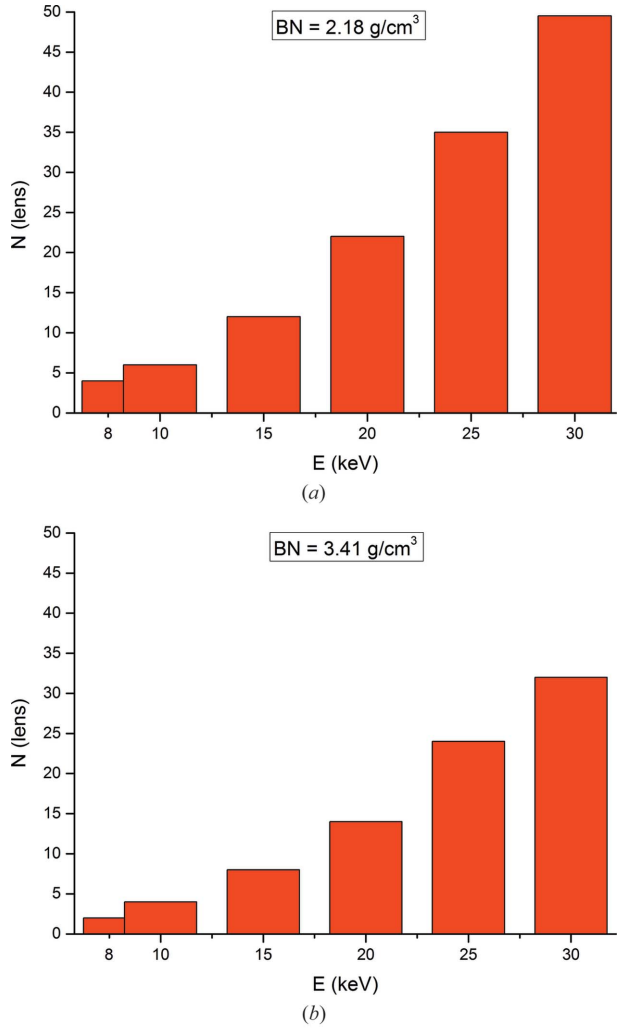

Figure 7
Required number of elementary lenses to reach 1 m focus distance at a certain energy: hexagonal modification of boron nitride with density 2.18 g cm^{-3} (*a*) and cubic modification of boron nitride with density 3.41 g cm^{-3} (*b*).

Nevertheless, materials with relatively large grain sizes can be applied in the methods of investigations using X-rays that are not sensitive to phase objects, like diffraction, reflectometry and others. In other cases it is reasonable to use materials with a grain size of less than 100 nm (Lyatun *et al.*, 2015) to minimize distortions of the wavefront of the X-ray beam caused by the material. However, the ideal materials for such applications can be single-crystal or amorphous glass-like materials which are free from X-ray diffuse scattering from grain boundaries, voids and inclusions. From this standpoint, single-crystal or amorphous glass-like materials based on Li, Be, B or C are of significant interest for further investigations.

5. Discussion and conclusion

In this work we have defined all major parameters which influence the material choice for X-ray refractive optics: the decrement of the refractive index, absorption coefficient, linear attenuation coefficient, density, refraction-to-attenua-

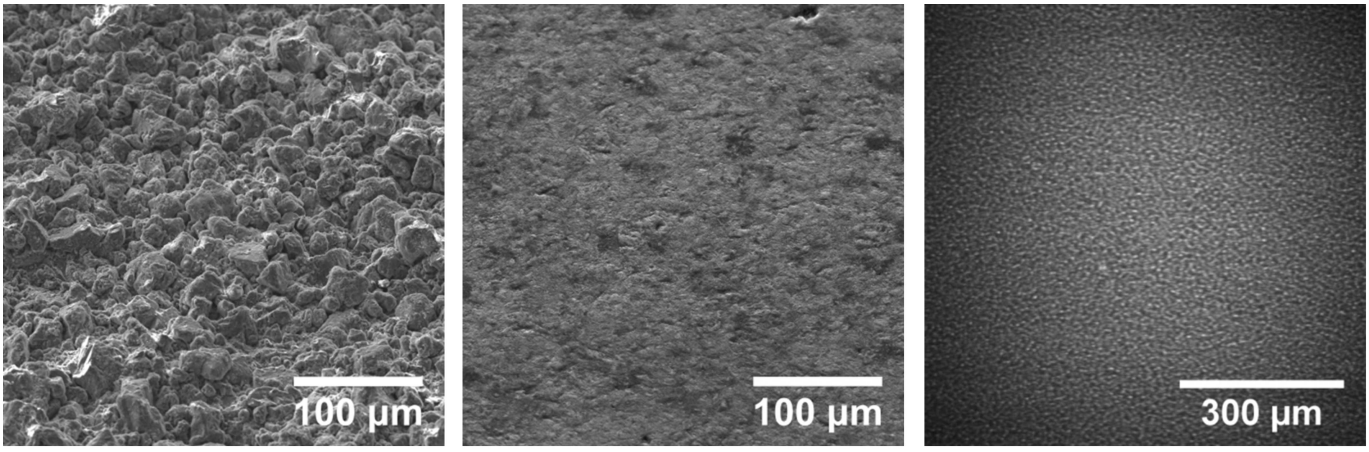

(*a*) (*b*) (*c*)

Figure 8
SEM images of the surface of the c-BN sample before polishing (*a*), after polishing (*b*) and its radiographic image at energy 14 keV (*c*).

tion ratio, number of lenses, effective aperture and refractive performance of the material. It turned out that only materials of the second and third periods of the periodic table can be used as a functional material for CRLs in the energy range 8–100 keV. From this standpoint, application of nickel lenses, for example, is not reasonable in this energy range. It was also shown that the presence of elements of the fourth (or higher) period has a fatal effect on the X-ray properties of a binary compound even with a high concentration of the second light element, like YB_{66}.

As follows from calculations, the optimal material for CRLs in the energy range 8–25 keV is beryllium, as long as it provides a significantly higher effective aperture than other materials. At higher energies the effective apertures of LiB, C, B_4C and c-BN become very similar to that of beryllium; at the same time diamond and cubic boron nitride require much fewer elementary lenses. As shown in Fig. 6, the refraction performance of C and c-BN is 2–2.5 times higher than that of beryllium starting from 30 keV. This result is of great importance. First of all, we may conclude that CRLs made of aluminium, silicon or nickel, which are widely used at synchrotron radiation sources, can be successfully replaced by CRLs made of diamond or cubic boron nitride insofar as they demonstrate higher optical performance. Secondly, C and c-BN lenses are perfect candidates for application at X-ray transfocators. Owing to high refraction, these materials could minimize the length of the lens assembly. It stands to reason that lens minimization can also reduce beam deviation behind the X-ray transfocator that may be caused by non-ideal lens shape, lens slope, mismatch of lens centers, *etc*.

Fortunately, both diamond and cubic boron nitride have highly symmetrical tetrahedral covalent bonding that makes these materials chemically stable and resilient to extra high thermal and radiation loading. For instance, the melting point of beryllium is 1562 K (Kleykamp, 2000), of cubic boron nitride is 3273 K (Pierson, 1996) and of diamond is ∼4000 K (Pierson, 1993). However, at high temperatures we should take into account the environment around the CRL. Thus, if oxygen is present, a black coating can form on the diamond surface starting from 900 K. In the case of an inert atmosphere the first stage of graphitization can be observed at 1800 K and rapidly increases to 2400 K. In turn, cubic boron nitride is extremely stable in air, nitrogen or vacuum up to 1673–1823 K (Landolt-Bornstein, 2002). Excellent thermal properties of diamond and cubic boron nitride together with high optical performance provide the possibility to take full advantages of the increased brilliance of X-ray beams at the new generation of synchrotron radiation sources and X-ray free-electron lasers.

With all the advantages of diamond and c-BN it should be noted that these materials have the highest hardness among all known materials at the moment. This means that the classic mechanical methods of lens fabrication are inefficient in this case. In the meantime, the perfection of the lens profile strongly affects the performance of CRLs. Nevertheless, some unique techniques have already demonstrated the possibility of successful treatment of such materials. Terentyev *et al.* (2015) report the successful manufacturing of parabolic single-crystal diamond lenses using laser ablation. In turn, at I. Kant BFU (Kaliningrad, Russia) it was shown that electrical discharge machining is a feasible method for boron nitride treatment.

Finally we presented the influence of the crystal structure on X-ray properties. It was shown that different phase modifications of the same material lead to density variation, which influence the refraction properties and transmission. In terms of refractive X-ray optics it is reasonable to use more dense modification in order to reduce the number of individual lenses in the CRL. In turn, to increase the transmission of X-ray windows, less dense modifications are preferable. Among the materials investigated in this work, LiB, Be and B_4C have the lowest linear attenuation coefficient; however, LiAl, α-hexagonal boron nitride and graphite may be considered as functional materials for X-ray windows at higher energies as well. Nevertheless, it is worth remarking on the significant role of the internal structure on potential

materials application. Only materials that are free of the X-ray diffuse scattering from grain boundaries, voids and inclusions can be used for refractive X-ray optics and X-ray windows. From this standpoint, single-crystal or amorphous glasslike materials based on Li, Be, B or C are of significant interest.

Acknowledgements

The work was supported by the Ministry of Education and Science of the Russian Federation (contract Nos. 14.Y26.31.0002 and 02.G25.31.0086).

References

Henke, B. L., Gullikson, E. M. & Davis, J. C. (1993). *At. Data Nucl. Data Tables*, **54**, 181–342.
Kleykamp, H. (2000). *Thermochim. Acta*, **345**, 179–184.
Kohn, V. G. (2003). *J. Exp. Theor. Phys.* **97**, 204–215.
Landolt-Bornstein. (2002). *Group VIII Advanced Materials and Technologies*, Vol. 2A2, pp. 13–93. Berlin Heidelberg: Springer-Verlag.
Lengeler, B., Schroer, C., Tummler, J., Benner, B., Richwin, M., Snigirev, A., Snigireva, I. & Drakopoulos, M. (1999). *J. Synchrotron Rad.* **6**, 1553–1167.
Lyatun, I. I., Goikhman, A. Yu., Ershov, P. A., Snigireva, I. I. & Snigirev, A. A. (2015). *J. Surface Investig.* **9**, 446–450.
Pierson, H. O. (1993). *Handbook of Carbon, Graphite, Diamond and Fullerenes: Properties, Processing and Applications*, p. 40. New Jersey: Noyes Publications.
Pierson, H. O. (1996). *Handbook of Refractory Carbides and Nitrides: Properties, Characteristics, Processing and Apps*, p. 236. New Jersey: Noyes Publications.
Schroer, C. G., Kuhlmann, M., Lengeler, B., Gunzler, T. F., Kurapova, O., Benner, B., Rau, C., Simionovici, A. S., Snigirev, A. A. & Snigireva, I. I. (2002). *Proc. SPIE*, **4783**, 10–18.
Snigirev, A., Kohn, V., Snigireva, I. & Lengeler, B. (1996). *Nature (London)*, **384**, 49–51.
Snigirev, A., Snigireva, I., Vaughan, G., Wright, J., Rossat, M., Bytchkov, A. & Curfs, C. (2009). *J. Phys. Conf. Ser.* **186**, 012073.
Solozhenko, V. (1995). *High. Press. Res.* **13**, 199–214.
Terentyev, S., Blank, V., Polyakov, S., Zholudev, S., Snigirev, A., Polikarpov, M., Kolodziej, T., Qian, J., Zhou, H. & Shvyd'ko, Y. (2015). *Appl. Phys. Lett.* **107**, 111108.
Tummler, J. (2000). PhD dissertation, RWTH Aachen, Germany.